

Docking Studies on Formylchromone Derivatives as Protein Tyrosine Phosphatase 1B (PTP1B) Inhibitors

Chan Kyung Kim,* Kyung A Lee, Hui Zhang, Hyeongjin Cho, and Bon-Su Lee

Department of Chemistry, Inha University, Incheon 402-751, Korea. *E-mail: kckyung@inha.ac.kr

Received March 22, 2007

Molecular modeling study has been performed to assist in the design of PTP1B inhibitors using FlexX. FlexX dockings with 19 test ligands, whose structures have been determined by X-ray crystallography, were successful in reproducing the experimental conformations within the protein. An increase in biological activity is observed as hydrophobic character of formylchromone derivatives increases. Most ligands bind to the active-site regions of the protein successfully in two different score runs. The Drug score run gave better results than the FlexX score run based on the score, rank, binding modes and bond distance of docked structures. Consensus values from the CScore scoring function are between 3 and 5, suggesting that the scoring scheme is reliable. All formylchromone inhibitors considered in this work show unidirectional binding modes in the active site pocket, which is contrary to the bidirectional X-ray results by Malamas *et al.* and amino acid residues responsible for such orientation are identified to help further development of the inhibitors.

Key Words : FlexX docking, PTP1B inhibitors, Formylchromone derivatives, Protein-ligand interaction, CScore

Introduction

A large part of signaling pathways inside the cell is regulated by phosphorylation of amino acid residues. The phosphorylation of a protein can create novel recognition mechanisms for protein-protein interaction, can control protein stability and, most importantly, can regulate enzyme activity.¹ Among them, phosphorylation of tyrosine residue is essential in regulating cellular metabolism, proliferation, differentiation, and oncogenic transformation. These reactions are catalyzed by two sets of enzymes, protein tyrosine kinases (PTKs) and protein tyrosine phosphatases (PTPs) (see Figure 1). PTKs operate in a synthetic way (phosphorylation) while PTPs catalyze the reverse (cleavage) reaction.² Abnormal functions of certain PTPs-dependent signal transduction are involved in a variety of diseases such as diabetes, obesity, autoimmune disease, infectious diseases, inflammation, cancer, osteoporosis and neurodegeneration.³ For this reason, development of effective inhibitors has been performed to design new therapeutics.

PTPs are hydrolysis enzymes that remove phosphate group from a phosphorylated tyrosine residue (pTyr). In spite of extensive studies on PTPs by many research groups, only little is known about their biological role. Since the discovery of the first PTP, many other family members have been identified, and the mammalian gene family is now known to have 90-100 members, as defined by their common ~250 amino acid catalytic domain.^{4,5} For PTPs a critical catalytic component is the active-site signature motif (H/V)C-X₅-R(S/T) (where X is any residue). This motif has been identified as being involved in the catalytic mechanism by numerous studies using site-directed mutagenesis, enzyme derivatization and isolation of catalytic intermediates.⁵ In the transition state for the initial phosphoryl transfer from the substrate to the PTP active site, cysteine (Cys) and arginine (Arg) play a dual role in both ground state stabilization and transition state stabilization. The general acid aspartic acid (Asp) is on the flexible loop that undergoes a substantial conformational change upon binding of substrate.

PTPs have been identified as novel therapeutic targets of

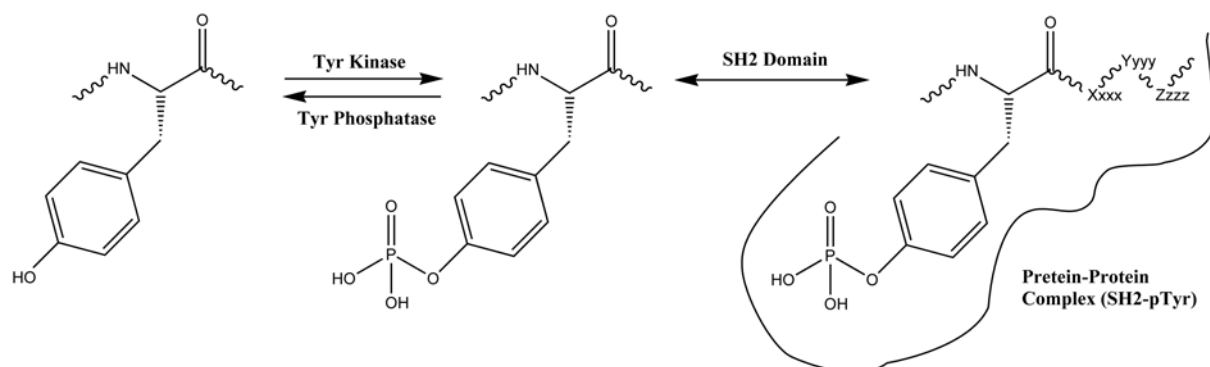


Figure 1. Schematic diagram for the action of protein tyrosine kinases (PTKs) and protein tyrosine phosphatases (PTPs).

insulin action in insulin-resistant disease. Insulin resistance in liver and peripheral tissues is a common cause of type II diabetes.⁶ Recent studies have proved that one of the important functions of the intracellular enzyme PTP1B is to suppress insulin action.⁷ Reduction of PTP1B not only enhances insulin sensitivity and improves glucose metabolism, but also protects against obesity induced by high-fat feeding.⁸ In another experiment, inhibition of PTP1B has shown enhanced insulin signaling in preclinical models. In the phosphorylation cascade, insulin receptor and insulin receptor substrate-1 (IRS1) have been implicated as substrates. Inhibition of PTP1B has been shown to stimulate kinase cascades. Therefore PTP1B inhibitors may play an important role in the treatment of type II diabetes.

As a continuing work on the computer-aided molecular design in our lab,^{9,10} molecular docking study has been carried out on a series of formylchromone derivatives¹¹ in order to find out the best binding conformations and orientations of these ligands against PTP1B.

Computational Approach

Structural Model for FlexX Docking Validation. Reproducing the binding conformation of a ligand whose crystal structure has already been solved is an important prerequisite for the docking study of unknown compounds. In order to accomplish this, seventeen ligand-protein complexes of PTP1B family were taken from the Protein Data Bank^{12,13} (pdb code = 1C83,¹⁴ 1C84,¹⁵ 1C85,¹⁵ 1C87,¹⁶ 1C88,¹⁶ 1ECV,¹⁵ 1L8G,¹⁷ 1NO6,¹⁸ 1Q1M,¹⁹ 1QXK,²⁰ 1XB0,²¹ 1BZJ,²² 1BZC,²² 1KAK,²³ 1KAV,²³ 1Q6J,²⁴ and 1Q6M²⁴). The PTP1Bs used in the X-ray structures can be classified into three groups based on their sequence identity – Group 1: 1C83, 1C84, 1C85, 1C87, 1C88, 1ECV, 1L8G, Group 2: 1NO6, 1Q1M, 1QXK, 1XB0, 1BZJ, 1KAK, 1KAV, 1Q6J, 1Q6M, Group 3: 1BZC. Two residues were different among three groups: Group 1 – Thr151, Asp252, Asp265; Group 2 – Ser151, Glu252; Group 3 – Ser151, Glu265. The ligands bound to the X-ray structures were sequentially labeled from **A** to **Q** (**A**: 6-(oxalyl-amino)-1H-indole-5-carboxylic acid, **B**: 3-(oxalyl-amino)-naphthalene-2-carboxylic acid, **C**: 2-(oxalyl-amino)-benzoic acid, **D**: 2-(oxalyl-amino)-4,7-dihydro-5H-thieno[2,3-C]pyran-3-carboxylic acid, **E**: 2-(oxalyl-amino)-4,5,6,7-tetrahydro-thieno[2,3-C]pyridine-3-carboxylic acid, **F**: 5-iodo-2-(oxalyl-amino)-benzoic acid, **G**: 7-(1,1-dioxo-1H-benzo[D]isothiazol-3-ylloxymethyl)-2-(oxalyl-amino)-4,7-dihydro-5H-thieno[2,3-C]pyran-3-carboxylic acid, **H**: 2-[(carboxycarbonyl)(1-naphthyl) amino]benzoic acid, **I**: 5-(2-fluoro-5-[3-(3-hydroxy-2-methoxycarbonyl-phenoxy)-propenyl]-phenyl)-isoxazole-3-carboxylic acid, **J**: 2-{4-[2-acetyl-amino-3-(4-carboxy methoxy-3-hydroxy-phenyl)-propionyl-amino]-butoxy}-6-hydroxy-benzoic acid methyl ester, **K**: 5-(3-{3-[3-hydroxy-2-(methoxycarbonyl)phenoxy]propenyl}-phenyl)-4-(hydroxymethyl)isoxazole-3-carboxylic acid, **L**: 6-(difluoro-phosphono-methyl)-naphthalene-2-carboxylic acid, **M**: 4-carbamoyl-4-{{6-(difluoro-phosphono-methyl)-naphthalene-2-carbonyl]-amino}-butyric acid, **N**: {{[7-(di-

fluoro-phosphono-methyl)-naphthalen-2-yl]-difluoro-methyl}-phosphonic acid, **O**: [(4-{4-[(difluoro-phosphono-methyl)-phenyl]-butyl]-phenyl)-difluoro-methyl]-phosphonic acid, **P**: [4-(2-(1H-1,2,3-benzotriazol-1-yl)-3-{4-[difluoro(phosphono)methyl]phenyl}-2-phenylpropyl)phenyl)(difluoro)methylphosphonic acid, **Q**: {[2-(1H-1,2,3-benzotriazol-1-yl)-2-(3,4-difluoro phenyl)propane-1,3-diy]bis[4,1-phenylene-(difluoromethylene)]}bis(phosphonic acid)). In these X-ray structures, two different types of inhibitors were cocrystallized with PTP1B: ligands **A-K** are carboxylic acids and ligands **L-Q** are phosphonic acids. All water molecules were deleted from the protein except in one case. Ligand **N** binds to 1KAK through a hydrogen bond with H₂O 433. 2D structures of these ligands are shown in Figure 2. In the crystal structures, the key functional group, -COO⁻ or -PO₃²⁻, extends deep into the active site of PTP1B, making several hydrogen bonds and hydrophobic interaction. Volumes of the ligands **A-Q** were calculated using van der Waals surface model.²⁵

Recently surprising X-ray structures of PTP1B with a benzothiophene biphenyl (**R**) and a sulfono biphenyl (**S**) (see Figure 2) were reported by Malamas and coworkers.²⁶ In their study, the orientations of large hydrophobic groups show opposite directionality in the active site of PTP1B. In the case of **R**, the large hydrophobic group points toward Lys120, Lys116 and Phe182 forming van der Waals interaction and we define such orientation as “left”. On the other hand, the large hydrophobic group of **S** forms nonspecific van der Waals interactions with the protein in opposite direction and this orientation is defined as “right”. Therefore, ligands **R** and **S** are also included in the docking study. All ligands having large hydrophobic groups (**G**, **I**, **J**, **K**, **M**, and **O**) show “right” orientation in the X-ray structures.

Geometries of test ligands **A-Q** were extracted from the corresponding PDB files and were minimized by using the Powell method with the standard TRIPOS force field/parameters in Sybyl 6.9 molecular modeling software²⁷ until an energy gradient of 0.05 kcal mol⁻¹ was reached.^{28,29} The atomic charges of all ligands were calculated using the Gasteiger-Hückel method.³⁰ Since no experimental structures were available for **R** and **S**, they were sketched using the sketch module in SYBYL 6.9 and each global minimum was selected from the grid search and then was used as a starting point for FlexX docking. In order to consider the effect of hydrophobicity in ligand-protein interaction, log P was computed using TRIPOS software.

FlexX docking set was composed of 36 formylchromone derivatives labeled **1** to **36** that have been shown to have antagonistic biological activity against PTP1B. The 2D chemical structures and biological data (expressed as IC₅₀, μM) of entire compounds¹¹ are tabulated in Table 1.

Docking. FlexX is a fast, flexible docking method that uses an incremental construction algorithm to place flexible ligands into a rigid active site and is known to perform well to reproduce X-ray structures.³¹ Standard parameters of the FlexX program as implemented in SYBYL 6.9 were used during docking.^{27,32} The residues within 10 Å to the bound

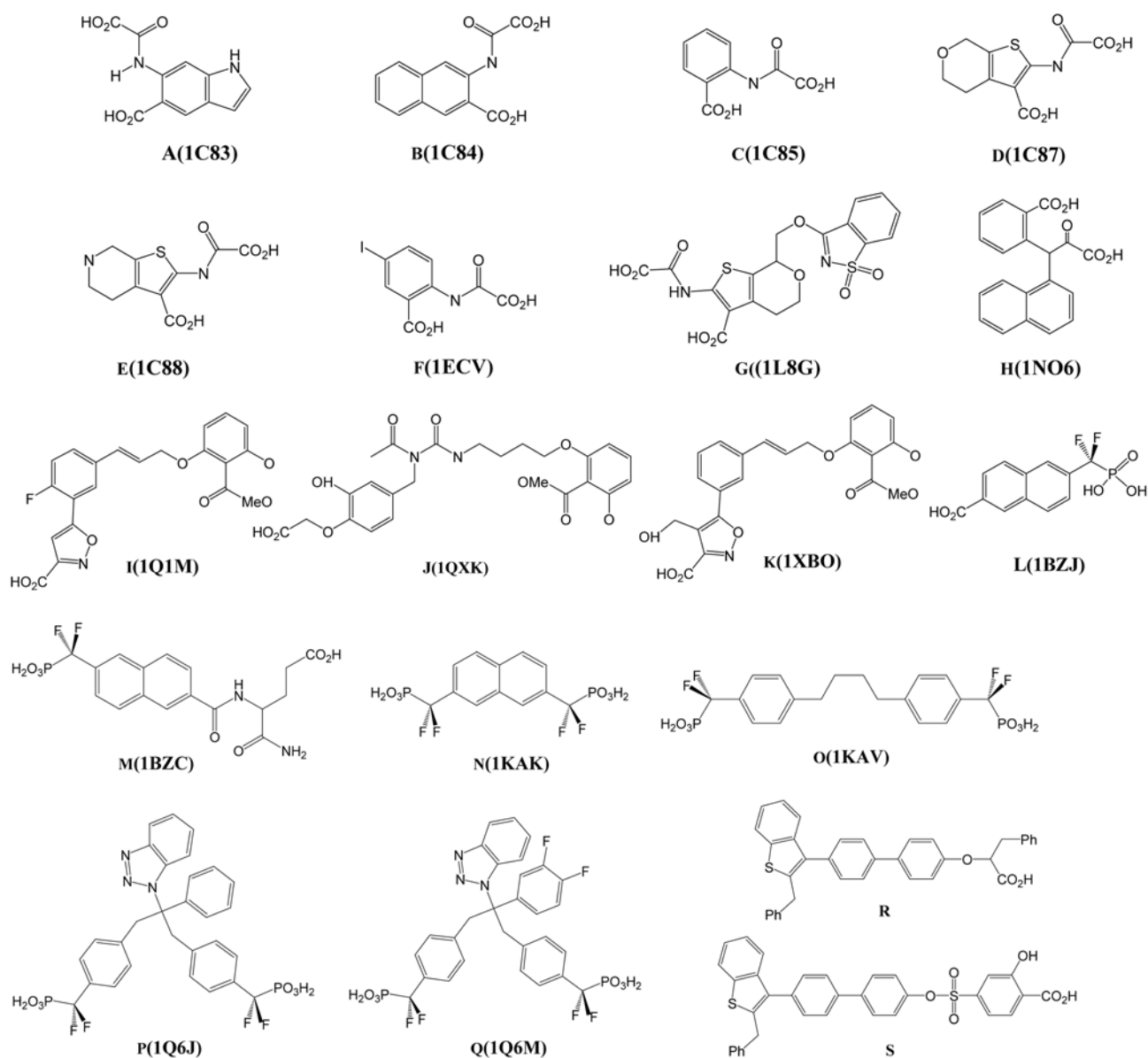
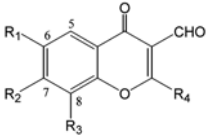


Figure 2. PTP1B inhibitors. All inhibitors are shown as the neutral species. Anionic forms were used in the docking. PDB code names to which these ligands were bound are shown in parentheses.

ligand were included in defining the active site for docking. Only Cys215 residue was selected as a subpocket. The use of a subpocket lets FlexX place the base fragment (the first placed fragment of the ligand) near one of the residues in the subpocket. All rotatable bonds were considered as flexible in the process of docking in order to identify the best binding conformation of a ligand with PTP1B. Bond lengths and angles were kept constants as given in the optimized structures.

The scoring function, which is optimized to reproduce experimental binding affinities, is used to estimate the binding free energy (ΔG_{bind}) of the protein-ligand complex. Two separate runs were tried using different scoring functions-FlexX score or Drug score.^{33,34} Additionally, Consensus score (CScore) was also calculated.³⁵ CScore is the counter of good results for each ligand in each scoring function –

F_{score} ,³² G_{score} ,³⁶ PMF score,³⁷ D_{score} ³⁸ and Chem score.³⁹ In each run, 50 poses were generated if possible and the poses were classified into two groups (see Table 2). If the key functional group (carboxylate, phosphonate or aldehyde group) points toward the subpocket, it is considered as “success” and the others as “failure”. Among “success” poses, the orientation of bulky hydrophobic group (or bulkier group if two groups are present) is classified further as “right” or “left” depending on its directionality in the active site. Such classification is not possible for inhibitors with small substituents (**A-F**, **H**, **L**, **N**, **1**, **~10**) or evenly distributed substituents (**P-Q**, **30**). Neither further minimization nor molecular dynamic simulations has been performed after the FlexX docking. As a representative case, the pose with the least root-mean-square-deviations (RMSD) was chosen as an optimal pose in FlexX score or Drug score run if the

Table 1. Structures and biological activities of 36 formylchromone derivatives


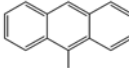
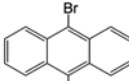
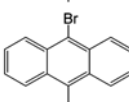
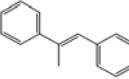
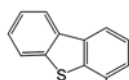
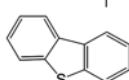
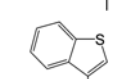
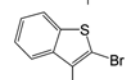
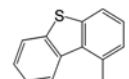
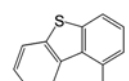
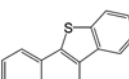
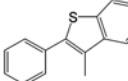
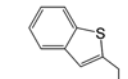
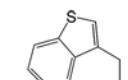
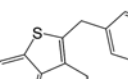
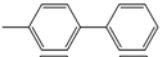
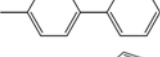
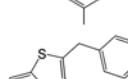
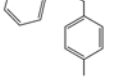
No.	R ₁	R ₂	R ₃	R ₄	IC ₅₀ (μM)	-logIC ₅₀
1	H	H	H	H	73.0	3.14
2	H	H	H	NH ₂	>1000	2.00
3	<i>iso</i> -C ₃ H ₇	H	H	H	22.0	3.66
4	Cl	H	H	H	28.0	3.55
5	Cl	H	Cl	H	25.0	3.60
6	Cl	CH ₃	H	H	18.0	3.74
7	Br	H	H	H	20.0	3.70
8	Br	H	Br	H	20.0	3.70
9	NO ₂	H	H	H	91.0	3.04
10	F	H	H	H	55.0	3.26
11		H	H	H	14.0	3.85
12	H	H		H	25.0	3.60
13		H	H	H	7.1	4.15
14		H	H	H	2.5	4.60
15		H	Br	H	11.0	3.96
16		H	H	H	9.7	4.01
17		H	H	H	10.9	3.96
18		H	Br	H	15.5	3.81
19		H	H	H	7.7	4.11
20		H	Br	H	8.2	4.09
21		H	H	H	7.6	4.12
22		H	Br	H	10.4	3.98
23		H	H	H	6.2	4.21

Table 1. Continued

No.	R ₁	R ₂	R ₃	R ₄	IC ₅₀ (μM)	-logIC ₅₀
24		H	Br	H	7.8	4.11
25		H	H	H	6.0	4.22
26		H	H	H	6.0	4.22
27		H	H	H	3.7	4.43
28	H	H		H	16.0	3.80
29		H	H	H	14.0	3.85
30		H		H	3.3	4.48
31		H	H	H	4.3	4.37
32		H		H	2.0	4.70
33		H	H	H	1.1	4.96
34		H		H	1.0	5.00
35		H	H	H	36.0	3.44
36	H	H		H	18.0	3.74

reference structure was available. If no experimental structure was available, the binding modes were checked visually and the first structure having correct interaction pattern with Cys215 was selected as the representative pose.

The top-scoring conformations showed better binding interactions with the active site residues than other solutions. SYBYL was used to generate dynamic hydrogen bonds between the docked ligand and the amino acid residues in the active site of the protein. The same software package was used to visualize the binding mode by generating fast Connolly-type MOLCAD surfaces.⁴⁰

Results and Discussion

Validation Using Test Ligands A-S. In order to test the performance of FlexX docking algorithm for ligand binding to PTP1Bs, we performed two separated validation tests. In

Table 2. Volume and binding patterns of PTP1B inhibitors depicted in Figure 1^a

Ligand	Volume (Å ³)	FlexX Score				Drug Score			
		Success	Failure	Right	Left	Success	Failure	Right	Left
A ^b	175.9	50	0	–	–	50	0	–	–
B ^b	193.9	22	28	–	–	40	10	–	–
C ^b	149.8	27	23	–	–	35	15	–	–
D ^b	187.8	14	36	–	–	31	39	–	–
E ^b	192.1	10	40	–	–	25	25	–	–
F ^b	178.7	33	17	–	–	50	0	–	–
G	329.5	50	0	50	0	50	0	50	0
H ^b	275.6	47	3	–	–	50	0	–	–
I	327.2	32	18	32	0	50	0	45	5
J	435.4	27	23	27	0	28	22	28	–
K	356.0	50	0	47	3	50	0	50	0
L ^b	204.5	50	0	–	–	50	0	–	–
M	312.7	50	0	50	0	50	0	50	0
N ^b	239.5	5	45	–	–	25	25	–	–
O	322.9	50	0	35	15	50	0	50	0
P ^c	491.1	48	2	–	–	50	0	–	–
Q ^c	493.9	50	0	–	–	50	0	–	–
R	–	15	35	0	15	0	50	0	0
S	–	50	0	50	0	50	0	50	0

^aSuccess has correct binding pattern between the key functional group of the ligand and core subpocket. Among successful poses, the orientation of bulky hydrophobic group is subdivided into two directions. See text for detail. ^bOrientation of small hydrophobic groups can not be classified. ^cOrientation of two large hydrophobic groups can not be classified.

Table 3. Biological activities and results of the best pose having the smallest RMSD^a for the inhibitors depicted in Figure 1

Ligand	K _i (μM)	FlexX Score			Drug Score		
		rank	score	RMSD	rank	score	RMSD
A	14.0	1	–42.0	0.81	1	–44.6	0.71
B	9.9	16	–34.4	0.69	9	–27.5	0.68
C	23.0	11	–38.2	0.65	6	–35.1	0.52
D	14.0	1	–48.0	0.48	4	–32.8	0.47
E	0.29	7	–33.7	0.56	3	–34.5	0.51
F	14.0	3	–47.9	0.43	11	–33.6	0.58
G	0.6	38	–44.6	0.74	7	–31.3	0.83
H	39.0	2	–39.9	0.75	1	–25.6	0.59
I	6.9	10	–20.1	1.50	19	–30.6	0.93
J	9.0	19	–17.4	2.80(0.91) ^b	42	–33.7	8.46(1.01) ^b
K	0.92	1	–17.5	0.94	1	–34.6	0.75
L	22.0	2	–45.3	0.41	1	–46.7	0.22
M	12.0	34	–17.7	1.28	11	–42.8	1.82
N	26.0 ^c	36	–17.6	1.51	9	–42.2	1.78
O	4.4 ^c	49	–22.5	2.48(0.49) ^d	36	–28.0	7.54(0.34) ^d
P	0.016	21	–24.5	1.42	9	–42.0	1.63
Q	0.013	16	–21.4	2.94(0.24) ^d	9	–41.6	2.58(0.19) ^d
R	0.095	–	–16.2	–	–	–	–
S	0.028	–	–24.3	–	–	–63.9	–

^aRMSD was obtained by comparing non-hydrogen atoms. ^bRMSD for non-hydrogen atoms of 4-carbomethoxy-3-hydroxy phenyl group. ^cIC₅₀. ^dRMSD for phenyl difluoro-methyl phosphonic acid group.

the first test, seventeen ligands (**A-Q**) selected from the PDB database were docked to the corresponding PTP1Bs. Docking results are summarized in Table 2 along with the

volumes of ligands **A-Q**. Inspection of Table 2 shows that the ligand volumes showed large variations: 149.8 (**C**)-493.9 Å³ (**Q**). The success ratio varied from 10 % to 100% among 50 poses per FlexX docking run but Drug score run gave better success ratio than FlexX score run. When the successful poses were classified further by the orientations of large hydrophobic groups, preference of right direction was observed, which is in consonant with experimental results. The poses with the smallest RMSD in reference to cocrystallized PTP1B inhibitors are summarized in Table 3. The RMSDs of the best poses are small (< 2.0 Å) except in three cases. The large RMSDs of **J**, **O** and **Q** are caused by the bulky hydrophobic groups attached to the tail portion of the ligands (*vide infra*). When only the carboxylate (**J**) or phosphonate (**O** and **Q**) part of the ligand was considered, the RMSDs became smaller (0.19-1.01 Å). Another important point to notice from Table 3 is that the best poses are not always at the top ranks in both FlexX and Drug score runs. In Figure 3, we have compared the best docked poses (in red) of ligands **G**, **H**, **K**, and **Q** with the conformations (in orange) found experimentally in the enzyme-ligand complexes. FlexX predicts that the conformations of the key functional groups located on the left lower corner of each picture in Figure 3 are very similar to those found experimentally. Large RMSD of ligand **Q** is caused by different torsional angles of carbon connecting phenyl difluoromethyl phosphonic tail –50.3° (exp.) vs. 148.8° (FlexX).

In order to test the performance of the scoring functions, each score from the best RMSD poses is plotted against the experimental affinity in Figure 4. Both plots showed random

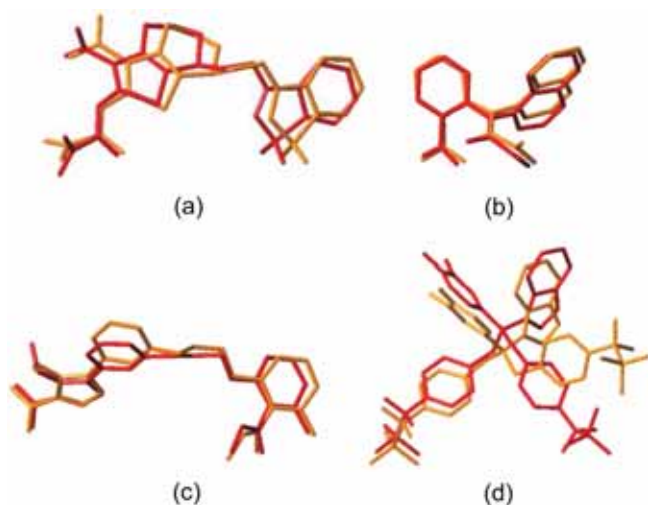


Figure 3. Comparison of docked (in red) and experimentally determined (in orange) conformations. (a) ligand **G**, (b) ligand **H**, (c) ligand **K**, (d) ligand **Q**.

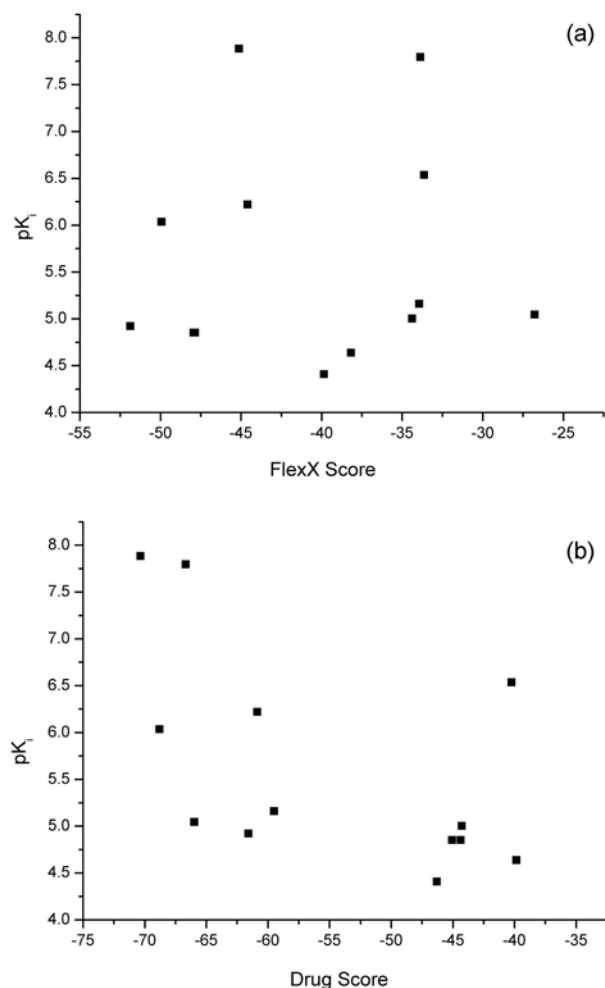


Figure 4. Plots of experimental affinities (pK_i) vs. FlexX score (a) and Drug score (b).

distribution of points, which suggests that it is hard to find a simple correlation for heterologous series of compounds.

In the second test, we performed the FlexX docking to

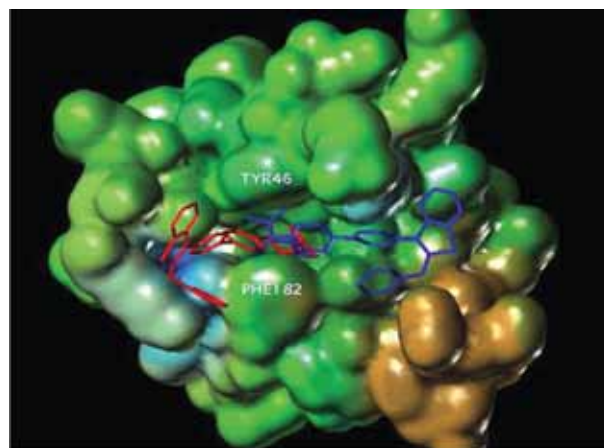


Figure 5. Schematic representation showing **R** (in red) and **S** (in blue) with key residues within the binding catalytic cavity.

verify the binding patterns of **R** and **S** against PTP1B. The X-ray structures were reported in the literature but the coordinates were not available from the PDB. In their X-ray structures, both carboxylate groups are extended deep into the active-site pocket occupying similar space and two water molecules form key hydrogen bonding interactions with the ligands. However, the orientations of hydrophobic groups are almost opposite in the active site as noted above. In the docking study, the coordinates of the protein was extracted from 1BZJ after removing the ligand **L**. All water molecules were also deleted from the protein because we had no information about their location. Many docking trials failed to find proper interaction pattern for ligand **R** (Table 2). 15 poses were docked correctly in FlexX score run but all trials were failed in Drug score run. Surprisingly, the orientations of the large hydrophobic group was invariably “left” as found in the X-ray structure. For ligand **S**, correct binding pattern was found for all 50 structures regardless of scoring functions. As a representative case, top-ranked pose of **R** (in red) or **S** (in blue) from FlexX score run is depicted in Figure 5. In this figure, MOLCAD surface was computed for the protein and was colored code by the lipophilicity (brown being very lipophilic, blue and green hydrophilic). From the above works, we have verified that the FlexX docking can reproduce the binding modes of key functional groups to PTP1B and can also give correct binding patterns for large hydrophobic groups regardless of the sizes of the ligands. Thus, we chose to use FlexX in subsequent analysis of binding of formylchromone inhibitors to the PTP1B.

Structural Properties of the Ligands. In Table 1, substituents on the formylchromone ring are classified as R_1 , R_2 , R_3 , and R_4 . Several important relationships were found between structures and biological activities: (1) IC_{50} value increases as the halogen atom at R_1 becomes more electro-negative (**10**, **4**, **7**). Similar increase in activity is also found for the halogen substituent at R_2 (**5**, **8**) but no cooperative effect is observed. (2) Introduction of NH_2 group at R_4 (**2**) results in marked decrease in inhibitory activity. (3) The unsubstituted analogues at R_3 are more active than the

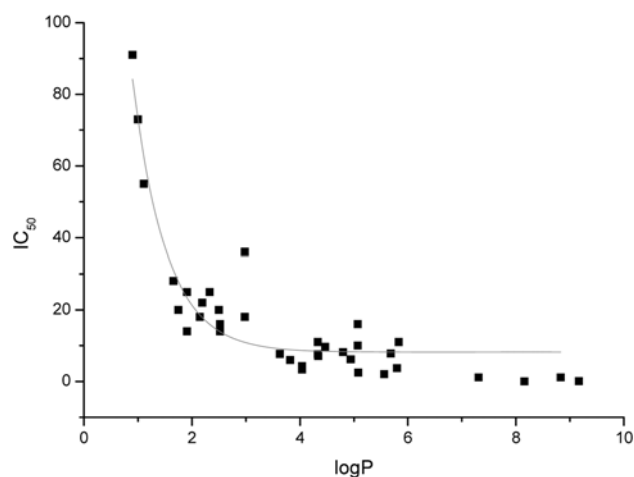


Figure 6. A plot of IC_{50} vs. $\log P$ for formylchromone derivatives.

corresponding Br-substituted analogues when the same benzothiophene groups are substituted at R_1 (**17** vs. **18**, **19** vs. **20**, **21** vs. **22**, and **23** vs. **24**). (4) The phenyl (**28**, **29**, **30**) and biphenyl analogues (**31**, **32**) are more active than the unsubstituted analogue, **1**. (5) The benzothiophene analogous compounds are found to be more potent against PTP1B when substituted at R_1 position.

In general, we found that bulkier hydrophobic group shows enhanced biological interaction with PTP1B. When $\log P$ values were plotted against IC_{50} (Figure 6), exponentially decreasing curve was observed. This suggests that hydrophobicity is a major component in determining biological activity of formylchromone derivatives.

FlexX Binding Models of Formylchromone Inhibitors.

From the validation work, we found that PTP1B has enough space in the active site to accommodate two different types of inhibitors. Since no crystallographic data were available for the binary complexes of formylchromone derivatives with PTP1B, molecular modeling study was carried out. The binding patterns of formylchromone derivatives against PTP1B are summarized in Table 4. From this Table, we can see that the success ratio is over 50% when 50 poses were obtained. This means that the inhibitors bind to the active-site pocket successfully in spite of simple definition of the active site. The analysis of binding pattern is also interesting for the inhibitors with large hydrophobic groups. Surprisingly, they all showed "right" preference, suggesting that van der Waals interaction between the hydrophobic group and the active-site residues is a major driving force for such directionality. In the X-ray structures by Malamas *et al.*,²⁶ however, no specific residues were mentioned except saying that the lipophilic 2-benzyl-benzothiophene tail-piece of ligand **S** formed nonspecific van der Waals contact with the protein. Characteristic score, rank and bond distance between aldehyde carbon and sulfur atom of Cys215, $d(C-S)$ of the best pose from each run are listed in Table 5. In this table, rank was recorded when a proper orientation between the aldehyde group and Cys215 residue appeared for the first time among 50 poses from each run. The ratios of finding higher ranks (between 1 and 5) were 56% and 86% for

Table 4. Binding patterns of formylchromone inhibitors considered in this work using FlexX^a

Ligand	FlexX Score				Drug Score			
	Success	Failure	Right	Left	Success	Failure	Right	Left
1	42	8	–	–	50	0	–	–
2^b	12	18	–	–	12	18	–	–
3	50	0	–	–	50	0	–	–
4	40	10	–	–	50	0	–	–
5	38	12	–	–	50	0	–	–
6	44	6	–	–	50	0	–	–
7	39	11	–	–	50	0	–	–
8	35	15	–	–	42	8	–	–
9	41	9	–	–	50	0	–	–
10	40	10	–	–	50	0	–	–
11	46	4	44	2	44	6	43	1
12	38	12	37	1	45	5	45	0
13	38	12	34	4	40	10	37	3
14	39	11	35	4	45	5	43	2
15	27	23	19	8	33	17	26	7
16^c	38	12	38	0	7	23	7	0
17	48	2	48	0	50	0	50	0
18	44	6	43	1	46	4	42	4
19	45	5	45	0	49	1	49	0
20	36	14	36	0	43	7	43	0
21	44	6	44	0	48	2	44	4
22	37	13	35	2	41	9	40	1
23	43	7	43	0	39	11	38	1
24	40	10	35	5	31	19	23	8
25	41	9	41	0	44	6	35	9
26	43	7	43	0	42	8	42	0
27	25	25	25	0	50	0	38	12
28	50	0	34	16	50	0	42	8
29	50	0	50	0	50	0	50	0
30	50	0	–	–	50	0	–	–
31	50	0	48	2	50	0	44	6
32	50	0	39	11	50	0	50	0
33	33	17	33	0	50	0	50	0
34	42	8	42	0	40	10	40	0
35	44	6	44	0	48	2	41	7
36	50	0	31	19	49	1	42	7

^asee footnote a in Table 2. ^bOnly 30 poses were recorded for both FlexX and Drug score run. ^cOnly 30 poses were found for Drug score run.

FlexX score run and Drug score run, respectively. The bond length, $d(C-S)$, was also included in Table 5 in order to check proper alignment of the aldehyde group with respect to Cys215. Based on the average C-S bond length ($3.55 \pm 0.33 \text{ \AA}$) for the experimental binary complexes containing ligands **A-K**, most compounds have reasonable C-S bond length (2.7 \AA – 5.0 \AA) necessary for the nucleophilic attack by sulfur atom. However, ligand **2** was unusual in many respects: i) It is only compound with a substituent, NH_2 , in R_4 position and its activity is the worst (Table 1). ii) In the FlexX run, only 30 poses were obtained and ratio of failure is the largest among the inhibitors (Table 2). iii) The top-scoring pose shows extraordinarily longer C-S bond length (Table 3). We

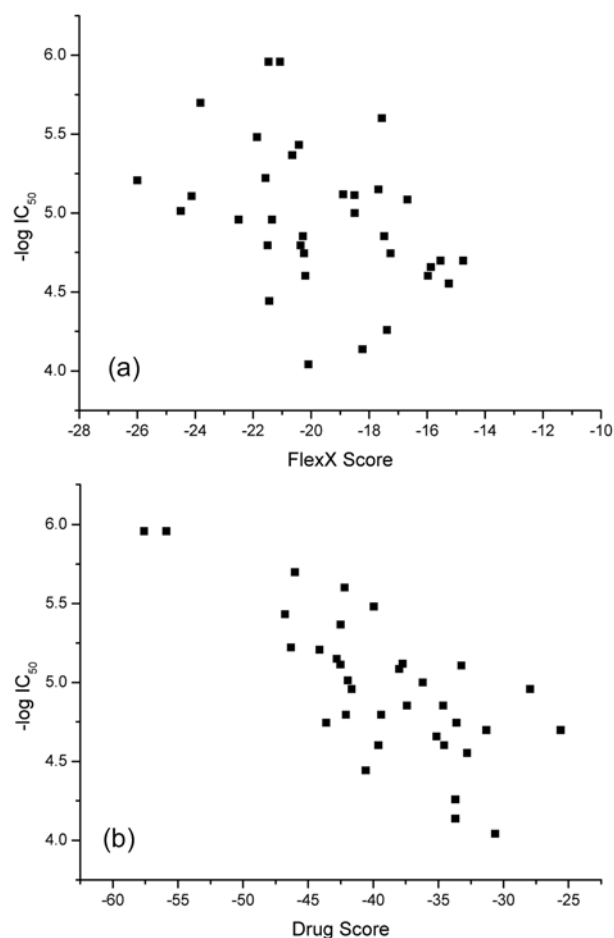
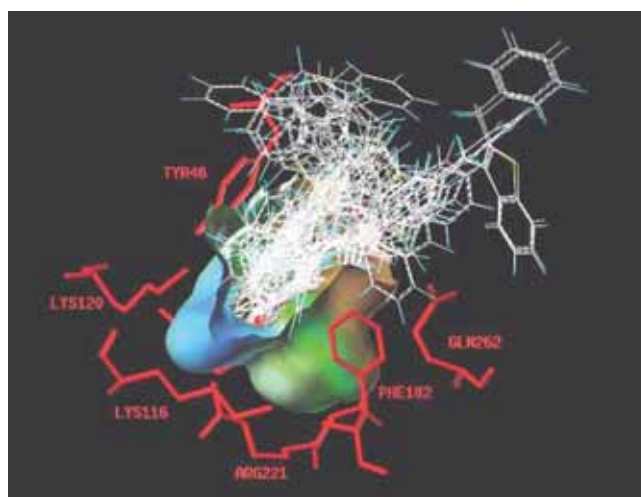
Table 5. Summary of the best pose having correct binding pattern between the inhibitor and core subpocket of the protein

Ligand	FlexX Score			Drug Score			CScore ^b
	rank	score	d(C-S) ^a	rank	score	d(C-S) ^a	
1	3	-18.2	3.22	1	-33.7	3.35	4
2	2	-12.0	6.39	1	-27.5	6.38	5
3	25	-15.9	3.97	3	-35.1	3.31	3
4	10	-15.3	2.73	1	-32.8	3.35	3
5	5	-16.0	2.73	1	-34.5	3.35	4
6	3	-17.3	2.83	1	-33.6	3.35	4
7	14	-14.8	2.73	1	-31.3	3.80	3
8	5	-15.5	2.73	1	-25.6	2.87	4
9	8	-20.1	2.73	6	-30.6	2.87	4
10	3	-17.4	3.22	1	-33.7	3.35	5
11	13	-17.5	3.08	4	-34.6	3.68	5
12	1	-20.2	3.22	1	-39.6	3.35	4
13	24	-17.7	3.28	1	-42.8	3.70	3
14	27	-17.6	3.28	1	-42.2	3.69	3
15	1	-22.5	4.90	9	-28.0	4.90	4
16	1	-24.5	5.02	2	-42.0	3.81	5
17	10	-21.4	2.74	1	-41.6	2.73	3
18	15	-20.4	2.74	1	-39.4	2.73	3
19	34	-18.5	3.02	1	-42.5	3.66	3
20	32	-16.7	3.98	1	-38.0	3.99	4
21	37	-18.9	3.12	2	-37.7	3.75	3
22	26	-18.5	3.83	1	-36.2	2.87	4
23	1	-26.0	5.01	1	-44.1	3.74	5
24	1	-24.1	5.02	9	-33.2	4.99	4
25	1	-21.6	5.02	1	-46.3	2.87	5
26	1	-21.6	5.01	2	-44.4	3.80	5
27	1	-20.4	4.57	5	-46.8	2.91	4
28	1	-21.5	3.03	1	-42.1	3.36	4
29	8	-20.3	2.83	3	-37.4	3.19	4
30	6	-21.9	2.94	9	-39.9	3.84	4
31	1	-20.7	2.83	1	-42.5	3.18	4
32	1	-23.8	2.95	2	-46.0	3.84	4
33	2	-21.5	2.83	2	-57.6	3.44	4
34	9	-21.1	2.97	6	-58.9	3.44	3
35	1	-21.4	5.06	2	-40.6	2.87	5
36	1	-20.3	2.99	1	-43.6	3.36	4

^adistance between aldehyde carbon of formylchromone derivatives and sulfur of Cys215 of the protein. ^bsum of the number of good results in each scoring function

have synthesized 5 more compounds with different substituents at this position (-NH-CO-Ph, -NH-CO-CH₂Ph, -NH-COCH₂CH₂Ph, NH-CH₂-COOC₂H₅, NH-CH₂-COOH) but all of them showed worse activity than **1**.

For formylchromone derivatives, total scores were -12 ~ -26 and -25 ~ -59 for the FlexX score run and Drug score run, respectively. Plots of -log IC₅₀ vs. FlexX score (or Drug score) depicted in Figure 7 show that *in vitro* activity increases as the score becomes more negative, but this trend is more evident for Drug score run. **2** was excluded in the plots. In general, we found that the docking by Drug score run were better than that from FlexX score run. Values of CScore

**Figure 7.** Plot of biological activity vs. total score. (a) -logIC₅₀ vs. FlexX score (b) -logIC₅₀ vs. Drug Score.**Figure 8.** Orientation of 35 formylchromone derivatives with top-scoring poses at the active site of PTP1B.

were over three in all cases, suggesting that the results could be considered good.

The best conformational poses of 35 inhibitors excluding **2** were superimposed on to the MOLCAD surface of the active site of PTP1B (Figure 8). Surprisingly, all top-scoring inhibitors are oriented toward “right” in the catalytic active

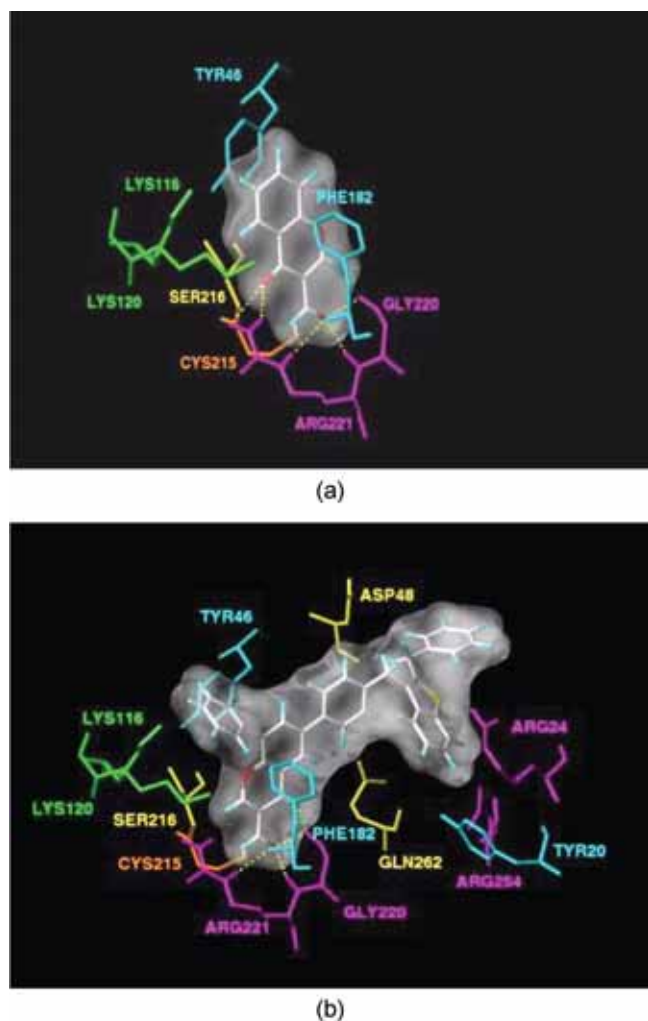


Figure 9. FlexX binding patterns of top-scoring poses of (a) **1** and (b) **34** with key residues at the active site of PTP1B.

site as found earlier in the X-ray structures. If so, what forces are responsible for the unidirectional orientation of hydrophobic groups of formylchromone derivatives? To answer this question, molecular interactions between top-scoring formylchromone inhibitors and the active-site residues were examined in detail. Compound **1**, which bears no substituents and **34**, which shows the highest biological activity are selected and compared as examples (Figure 9). From this figure, we can find that the aldehyde groups of formylchromone derivatives are extended deep into the active-site pocket. The aldehyde oxygen atom of **1** forms three hydrogen bonds with Gly220 (2.34 Å) and Arg221 (1.93 Å and 1.96 Å) and the same functional group of **34** forms hydrogen bond with Arg221 (1.91 Å and 2.72 Å). Additional hydrogen bonds exist between carbonyl oxygen and Arg221 (**1**) or Gly220 (**34**). The phenyl ring of the formylchromone skeleton is sandwiched between residues Tyr46 and Phe182. Such interaction patterns were also discovered experimentally. Five key residues are found to have close contacts with the large hydrophobic group of **34**: NH_3^+ groups of Arg24 and Arg254 with benzothiophene ring, backbone carbonyl oxygen of Asp48 with benzyl hydrogen, alkyl side

chain of Val49 with phenyl ring attached to formylchromone ring (not shown in Figure 9) and alkyl side chain of Met258 with benzyl group (not shown in Figure 9). Note that the formyl carbon atom of **1** and **34** positioned 3.35 Å and 3.44 Å away from the sulfur of Cys215, respectively, facilitating nucleophilic attack to form S-C bond.

Conclusions

FlexX docking studies have been performed to study binding patterns of a series of formylchromone derivatives against PTP1B. To test performance of FlexX module, 19 test ligands whose volumes changed from 149.8 to 493.9 Å³ were tried and compared with their X-ray structures. The top-scoring poses were surprisingly good in reproducing experimental structures. The orientation of lipophilic groups of **R** and **S**, which showed opposite orientations at the active-site pocket was also verified by the FlexX docking. Two types of scores – FlexX score and Drug score – were used to run Run-Multiple Ligand option of FlexX to get 50 conformations for each run. Successful binding of the aldehyde group of formylchromone derivatives to Cys215 were found in most cases. From the top-scoring structures of each FlexX run, we can propose the binding behavior of the inhibitors at the active site. The orientation of large hydrophobic group (or larger hydrophobic group) is the same as those found for most inhibitors experimentally. The residues responsible for such orientation are identified and can be used to design more compounds with enhanced activities.

Acknowledgement. This work was supported by INHA UNIVERSITY Research Grant.

References

- (a) Zhan, X.-L.; Wishart, M. J.; Guan, K.-L. *Chem. Rev.* **2001**, *101*, 2477. (b) Östman, A.; Böhrner, F. D. *Trends Cell Biol.* **2001**, *11*, 258. (c) Cohen, P. *Trends Biochem. Sci.* **2000**, *25*, 596. (d) Neel, B. G.; Tonks, N. K. *Curr. Opin. Cell Biol.* **1997**, *9*, 193.
- (a) Tonks, N. K.; Neel, B. G. *Curr. Opin. Cell Biol.* **2001**, *13*, 182. (b) Denu, J. M.; Dixon, J. E. *Curr. Biol.* **1998**, *2*, 633. (c) Zhang, Z.-Y. *Curr. Opin. Chem. Biol.* **2001**, *5*, 416.
- (a) Van Huijsduijnen, R. H.; Bombrun, A.; Swinnen, D. *Drug Discov. Today* **2002**, *7*, 1013. (b) Li, L.; Dixon, J. E. *Semin. Immunol.* **2000**, *12*, 75.
- Tonks, N. K.; Charbonneau, H.; Diltz, C. D.; Fischer, E. H.; Walsh, K. A. *Biochemistry* **1998**, *27*, 8695.
- Lander, E. S.; Linton, L. M.; Birren, B.; Nusbaum, C.; Zody, M. C.; Baldwin, J.; Devon, K.; Dewar, K.; Doyle, M.; FitzHugh, W.; Funke, R.; Gage, D.; Harris, K.; Heaford, A.; Howland, J.; Kann, L.; Lehoczky, J.; LeVine, R.; McEwan, P.; McKernan, K.; Meldrim, J.; Mesirov, J. P.; Miranda, C.; Morris, W.; Naylor, J.; Raymond, C.; Rosetti, M.; Santos, R.; Sheridan, A.; Sougnez, C.; Stange-Thomann, N.; Stojanovic, N.; Subramanian, A.; Wyman, D.; Rogers, J.; Sulston, J.; Ainscough, R.; Beck, S.; Bentley, D.; Burton, J.; Clee, C.; Carter, N.; Coulson, A.; Deadman, R.; Deloukas, P.; Dunham, A.; Dunham, I.; Durbin, R.; French, L.; Grafham, D.; Gregory, S.; Hubbard, T.; Humphray, S.; Hunt, A.; Jones, M.; Lloyd, C.; McMurray, A.; Matthews, L.; Mercer, S.; Milne, S.; Mullikin, J. C.; Mungall, A.; Plumb, R.; Ross, M.; Shownkeen, R.; Sims, S.; Waterston, R. H.; Wilson, R. K.; Hillier, L. W.; McPherson, J. D.; Marra, M. A.; Mardis, E. R.; Fulton, L.

- A.; Chinwalla, A. T.; Pepin, K. H.; Gish, W. R.; Chissoe, S. L.; Wendl, M. C.; Delehaunty, K. D.; Miner, T. L.; Delehaunty, A.; Kramer, J. B.; Cook, L. L.; Fulton, R. S.; Johnson, D. L.; Minx, P. J.; Clifton, S. W.; Hawkins, T.; Branscomb, E.; Predki, P.; Richardson, P.; Wenning, S.; Slezak, T.; Doggett, N.; Cheng, J. F.; Olsen, A.; Lucas, S.; Elkin, C.; Uberbacher, E.; Frazier, M.; Gibbs, R. A.; Muzny, D. M.; Scherer, S. E.; Bouck, J. B.; Sodergren, E. J.; Worley, K. C.; Rives, C. M.; Gorrell, J. H.; Metzker, M. L.; Naylor, S. L.; Kucherlapati, R. S.; Nelson, D. L.; Weinstock, G. M.; Sakaki, Y.; Fujiyama, A.; Hattori, M.; Yada, T.; Toyoda, A.; Itoh, T.; Kawagoe, C.; Watanabe, H.; Totoki, Y.; Taylor, T.; Weissbach, J.; Heilig, R.; Saurin, W.; Artiguenave, F.; Brottier, P.; Bruls, T.; Pelletier, E.; Robert, C.; Wincker, P.; Smith, D. R.; Doucette-Stamm, L.; Rubenfield, M.; Weinstock, K.; Lee, H. M.; Dubois, J.; Rosenthal, A.; Platzer, M.; Nyakatura, G.; Taudien, S.; Rump, A.; Yang, H.; Yu, J.; Wang, J.; Huang, G.; Gu, J.; Hood, L.; Rowen, L.; Madan, A.; Qin, S.; Davis, R. W.; Federspiel, N. A.; Abola, A. P.; Proctor, M. J.; Myers, R. M.; Schmutz, J.; Dickson, M.; Grimwood, J.; Cox, D. R.; Olson, M. V.; Kaul, R.; Raymond, C.; Shimizu, N.; Kawasaki, K.; Minoshima, S.; Evans, G. A.; Athanasiou, M.; Schultz, R.; Roe, B. A.; Chen, F.; Pan, H.; Ramsay, J.; Lehrach, H.; Reinhardt, R.; McCombie, W. R.; de la Bastide, M.; Dedhia, N.; Blocker, H.; Hornischer, K.; Nordsiek, G.; Agarwala, R.; Aravind, L.; Bailey, J. A.; Bateman, A.; Batzoglu, S.; Birney, E.; Bork, P.; Brown, D. G.; Burge, C. B.; Cerutti, L.; Chen, H. C.; Church, D.; Clamp, M.; Copley, R. R.; Doerks, T.; Eddy, S. R.; Eichler, E. E.; Furey, T. S.; Galagan, J.; Gilbert, J. G.; Harmon, C.; Hayashizaki, Y.; Haussler, D.; Hermjakob, H. *Nature* **2001**, *409*, 860.
6. (a) Zick, Y. *Trends Cell Biol.* **2001**, *11*, 437. (b) Bailey, C. *J. Biochem. Pharm.* **1999**, *58*, 1511. (c) Taylor, S. I. *Cell* **1999**, *97*, 9. (d) Kido, Y.; Burks, D. J.; Withers, D.; Bruning, J. C.; Kahn, C. R.; White, M. F. *J. Clinical Invest.* **2000**, *105*, 199. (e) Cheng, A.; Dubé, N.; Gu, F.; Tremblay, M. L. *Eur. J. Biochem.* **2002**, *269*, 1050.
7. (a) Elchebly, M.; Payette, P.; Michaliszyn, E.; Cromlish, W.; Collins, S.; Loy, A. L.; Normandin, D.; Cheng, A.; Himms-Hagen, J.; Chan, C. C.; Ramachandran, C.; Gresser, M. J.; Tremblay, M. L.; Kennedy, B. P. *Science* **1999**, *283*, 1544. (b) Klamann, L. D.; Boss, O.; Peroni, O. D.; Kim, J. K.; Martino, J. L.; Zabotny, J. M.; Moghal, N.; Lubkin, M.; Kim, Y.-B.; Sharpe, A. H.; Stricket-Krongrad, A.; Shulman, G. I.; Neel, B. G.; Kahn, B. B. *Mol. Cell Biol.* **2000**, *20*, 5479.
8. (a) Zinker, B. A.; Rondinone, C. M.; Trevillyan, J. M.; Gum, R. J.; Clampit, J. E.; Waring, J. F.; Xie, N.; Wilcox, D.; Jacobson, P.; Frost, L.; Kroeger, P. E.; Reilly, R. M.; Koterski, S.; Oppenorth, T. J.; Ulrich, R. G.; Crosby, S.; Butler, M.; Murray, S. F.; Mckay, R. A.; Bhanot, S.; Monia, B. P.; Jirousek, M. R. *Proc. Natl. Acad. Sci. U.S.A.* **2002**, *99*, 11357. (b) Rondinone, C. M.; Trevillyan, J. M.; Clampit, J.; Gum, R. J.; Berg, C.; Kroeger, P.; Frost, L.; Zinker, B. A.; Reilly, R.; Ulrich, R.; Butler, M.; Monia, B. P.; Jirousek, M. R.; Waring, J. F. *Diabetes* **2002**, *51*, 2405. (c) Ramachandran, C.; Kennedy, B. P. *Curr. Top. Med. Chem.* **2003**, *3*, 749.
9. Lee, D. Y.; Hyun, K. H.; Park, H. Y.; Lee, B.-S.; Kim, C. K. *Bull. Korean Chem. Soc.* **2006**, *27*, 273.
10. Lee, I. Y.; Lee, K. A.; Lee, B.-S.; Chi, D. Y.; Kim, C. K. *Bull. Korean Chem. Soc.* **2006**, *27*, 1969.
11. (a) Shim, Y. S.; Kim, K. C.; Chi, D. Y.; Lee, K.-H.; Cho, H. *Bioorg. Med. Chem. Lett.* **2003**, *13*, 2561. (b) Shim, Y. S.; Kim, K. C.; Lee, K. A.; Shrestha, S.; Lee, K.-H.; Kim, C. K.; Cho, H. *Bioorg. Med. Chem.* **2005**, *13*, 1325.
12. Berman, H. M.; Wilson, I. B. *J. Biol. Chem.* **1962**, *237*, 3245.
13. PDB files are downloadable from <http://www.rcsb.org/pdb>
14. Groves, M. R.; Yao, Z.-J.; Burke, T. R. Jr.; Barford, D. *Biochemistry* **1998**, *37*, 17773.
15. Andersen, H. S.; Iversen, L. F.; Jeppesen, C. B.; Branner, S.; Norris, K.; Rasmussen, H. B.; Moller, K. B.; Moller, N. P. *J. Biol. Chem.* **2000**, *275*, 7101.
16. Iversen, L. F.; Andersen, H. S.; Branner, S.; Mortensen, S. B.; Peters, G. H.; Norris, K.; Olsen, O. H.; Jeppesen, C. B.; Lundt, B. F.; Ripka, W.; Moller, K. B.; Moller, N. P. *J. Biol. Chem.* **2000**, *275*, 10300.
17. Iversen, L. F.; Andersen, H. S.; Moller, K. B.; Olsen, O. H.; Peters, G. H.; Branner, S.; Mortensen, S. B.; Hansen, T. K.; Lau, J.; Ge, Y.; Holsworth, D. D.; Newman, M. J.; Moller, N. P. *Biochemistry* **2001**, *40*, 14812.
18. Szczepankiewicz, B. G.; Liu, G.; Hajduk, P. J.; Abad-Zapatero, C.; Pei, Z.; Xin, Z.; Lubben, T.; Trevillyan, J. M.; Stashko, M. A.; Bballaron, S. J.; Liang, H.; Huang, F.; Hutchins, C. W.; Fesik, S. W.; Jirousek, M. R. *J. Am. Chem. Soc.* **2003**, *125*, 4087.
19. Liu, G.; Xin, Z.; Pei, Z.; Hajduk, P. J.; Abad-Zapatero, C.; Hutchins, C. W.; Zhao, H.; Lubben, T. H.; Ballaron, S. J.; Haasch, D. L.; Kaszubska, W.; Rondinone, C. M.; Trevillyan, J. M.; Jirousek, M. R. *J. Med. Chem.* **2003**, *46*, 4232.
20. Xin, Z.; Liu, G.; Abad-Zapatero, C.; Pei, Z.; Szczepankiewicz, B. G.; Li, X.; Zhang, T.; Hutchins, C. W.; Hajduk, P. J.; Ballaron, S. J.; Stashko, M. A.; Lubben, T. H.; Trevillyan, J. M.; Jirousek, M. R. *Bioorg. Med. Chem. Lett.* **2003**, *13*, 3947.
21. Zhao, H.; Liu, G.; Xin, Z.; Serby, M.; Pei, Z.; Szczepankiewicz, B. G.; Hajduk, P. J.; Abad-Zapatero, C.; Hutchins, C. W.; Lubben, T. H.; Ballaron, S. J.; Hassach, D. L.; Kaszubska, W.; Rondinone, C. M.; Trevillyan, J. M.; Jirousek, M. R. *Bioorg. Med. Chem. Lett.* **2004**, *14*, 5543.
22. Groves, M. R.; Yao, Z. J.; Roller, P. P.; Jr Bruke, T. R.; Barford, D. *Biochemistry* **1998**, *37*, 17773.
23. Jia, Z.; Ye, Q.; Dinaut, A. N.; Wang, Q.; Waddleton, D.; Payette, P.; Ramachandran, C.; Kennedy, B.; Hum, G.; Taylor, S. D. *J. Med. Chem.* **2001**, *44*, 4584.
24. Scapin, G.; Patel, S. B.; Becker, J. W.; Wang, Q.; Desponts, C.; Waddleton, D.; Skorey, K.; Cromlish, W.; Bayly, C.; Therien, M.; Gauthier, J. Y.; Li, C. S.; Lau, C. K.; Ramachandran, C.; Kennedy, B. P.; Asante-Appiah, E. *Biochemistry* **2003**, *42*, 11451.
25. Kim, C. K.; Lee, K. A.; Hyun, K. H.; Park, H. J.; Kwack, I. Y.; Kim, C. K.; Lee, H. W.; Lee, B.-S. *J. Comput. Chem.* **2004**, *25*, 2073.
26. Malamas, M. S.; Sredy, J.; Moxham, C.; Katz, A.; Xu, W.; McDevitt, R.; Adebayo, F. O.; Sawicki, D. R.; Seestaller, L.; Sullivan, D.; Taylor, J. R. *J. Med. Chem.* **2000**, *43*, 1293.
27. SYBYL 6.9; TRIPOS Inc.: St Louis, USA.
28. Powell, M. J. D. *Mathematical Programming* **1977**, *12*, 241.
29. (a) Clark, M.; Crammer, R. D.; Opdenbosch, N. V. *J. Comp. Chem.* **1989**, *10*, 982. (b) Dixon, D. A.; Zeroka, D. J.; Wendoloski, J. J.; Wasserman, Z. R. *J. Phys. Chem.* **1985**, *89*, 5334.
30. (a) Streitwieser, A. *Molecular Orbital Theory for Organic Chemists*; Wiley: NY, 1961. (b) Purcel, W. P.; Singer, J. A. *J. Chem. Eng. Data* **1967**, *12*, 235.
31. Hoffmann, D.; Kramer, B.; Washio, T.; Steinmetzer, T.; Rarey, M.; Lengauer, T. *J. Med. Chem.* **1999**, *42*, 4422.
32. Szczepankiewicz, B. G.; Liu, G.; Hajduk, P. J.; Abad-Zapatero, C.; Pei, Z.; Xin, Z.; Lubben, T.; Trevillyan, J. M.; Stashko, M. A.; Ballaron, S. J.; Linag, H.; Huang, F.; Hutchins, C. W.; Fesik, S. W.; Jirousek, M. R. *J. Am. Chem. Soc.* **2003**, *125*, 4087.
33. (a) Bohm, H. J. *J. Comput. Aided Mol. Des.* **1994**, *8*, 243. (b) Klebe, G. *J. Mol. Biol.* **1994**, *237*, 212.
34. Gohlke, H.; Hendlich, M.; Klebe, G. *J. Mol. Biol.* **2000**, *295*, 337.
35. Clark, R. D.; Strizhev, A.; Leonard, J. M.; Blake, F. F.; Matthew, J. B. *J. Mol. Graph. Modelling* **2002**, *20*, 281.
36. Jones, G.; Willett, P.; Glen, R. C.; Leach, A. R.; Taylor, R. *J. Mol. Biol.* **1997**, *267*, 727.
37. Muegge, I.; Martin, Y. C.; Hajduk, P. J.; Fesik, S. W. *J. Med. Chem.* **1999**, *42*, 2398.
38. Kuntz, I. D.; Blaney, J. M.; Oatley, S. J.; Langridge, R. L.; Ferrin, T. E. *J. Mol. Biol.* **1982**, *161*, 269.
39. Eldridge, M. D.; Murray, C. W.; Auton, T. R.; Paolini, G. V.; Mee, R. P. *J. Comput. Aided Mol. Des.* **1997**, *11*, 425.
40. (a) Connolly, M. L. *J. Appl. Crystallogr.* **1983**, *16*, 548. (b) Lorensen, W.; Cline, H. *Computer Graphics* **1987**, *21*, 163. (c) Heiden, W.; Goetze, T.; Brickmann, J. *J. Comput. Chem.* **1993**, *14*, 246.